

Mechanical and wear properties of Cu-Al-Ni-Fe-Sn-based alloy

Mitsuhiro Okayasu^{*1}, Daiki Izuka², Yushi Ninomiya¹,
Yuki Manabe³ and Tetsuro Shiraishi¹

¹Department of Materials Science and Engineering, Ehime University,
3 Bunkyo-cho, Matsuyama, Ehime, 790-8577, Japan

²Department of Machine Intelligence and Systems Engineering, Akita Prefectural University,
84-4 Aza Ebinokuchi, Tsuchiya, Yurijonjo, Akita, 015-0055, Japan

³Dozen-Kogyo Co. Ltd., 377 Naranoki, Saijyo, Ehime, 793-0065, Japan

(Received May 16, 2013, Revised September 10, 2013, Accepted November 18, 2013)

Abstract. To obtain bronze with good mechanical properties and high wear resistance, a new bronze (CADZ) is proposed on the basis of various fundamental information. The CADZ consists of the elements Al10.5, Fe4.2, Sn3.7 and Ni3.1, and its design is based on Cu-Al10.5 alloy. The Cu-10.5%Al is very hard and brittle. To obtain the high material ductility of the Cu-10.5%Al alloy, an attempt was made to add a few percent of Sn. Moreover, to make high strength of the Cu alloy, microstructure with small grains was created by the proper amount of Fe and Ni (Fe/Ni = 0.89). The mechanical properties of the CADZ sample have been examined experimentally, and those were compared with commercial bronzes. The tensile strength and wear resistance of CADZ are higher than those for commercial bronzes. Although the ductility of CADZ is the lower level, the strain to failure of CADZ is about 2.0~5.0% higher than that for the Cu-Al10.5 alloy. Details of the microstructural effects on the mechanical properties in the CADZ sample were further discussed using various experimental results.

Keywords: bronze; tensile property; fatigue property; wear property; microstructure

1. Introduction

There are various bronzes produced by the casting process. Bronzes have been employed for various engineering applications, as they have adequate ductility, good corrosion resistance and high hardness. The high mechanical properties confer good bearing properties due to good sliding and high wear resistance involving impact or shock loading. The excellent properties of bronzes, comparing favorably with carbon steels and cast irons, make them versatile engineering materials (Li *et al.* 1996). With additions of Mn and Si to bronze, particles of manganese silicide (Mn₅Si₃) are created, which lead to high hardness and high wear resistance (Waheed and Ridley 1996).

It is well known that aluminum bronze has excellent physical, hardness and tribological properties. Bronze with about 10%Al shows the better comprehensive properties and is among the most widely employed materials in the aluminum bronze family (Li *et al.* 2006). Al-bronze has been widely used for many engineering applications, such as in places requiring high corrosion

*Corresponding author, Ph.D., E-mail: mitsuhiro.okayasu@utoronto.ca

resistance and high strength. Those bronzes find applications in the automobile parts, marine equipment, pumps, valves, winches and their gears (Waheed and Ridley 1996). These alloys contain 8~14%Al and approximately 2~4%Mn, Ni and Fe (Kaplan and Yildiz 2003). The alloys contain the high hardness intermetallic compound $(\text{Ni,Fe})_3\text{Al}$ (Adabavazeh *et al.* 2012). An attempt has been made by Kaplan *et al.* to produce the aluminum bronze material $(\text{Cu-Ni}_4\text{-Al}_9\text{-Fe}_4)$ in a sand and metal mold; and the effects of casting condition, solution treatment and tempering heat treatment on the microstructures and mechanical properties were investigated (Kaplan and Yildiz 2003). From their approach, the highest mechanical properties (hardness, toughness and elasticity) of any Al-bronzes were obtained (Kaplan and Yildiz 2003). Turhan has examined the effect of Fe, Mn and P on the wear resistance of the bronzes. One of his conclusions is that the samples containing P showed the best abrasive wear resistance, but Fe and Mn elements reduced the wear resistance due to the formation of intermetallic compounds (Turhan 2005).

Our literature survey has revealed that good material properties and high wear resistance of bronzes are influenced by several elements, including Al, Sn, Ni and Fe. Some related bronzes have been proposed and standardized in the Japan Industrial Standard (JIS) including Cu-Fe-Ni-Al-Mn-, Cu-Sn-P- and Cu-Sn-based bronzes. Although several elements, e.g., Al, Sn, Fe and Ni, are important for producing good mechanical properties and high wear resistance, the details of the microstructural effects have not yet to be clearly reported. In addition, the bronzes have been used for linear and bearing parts in steel industries in Japan, but their lives are reported to be only 4~6 month due to the low wear resistance. The aim of this work is hence to propose a new bronze to have high fatigue strength and high wear strength. In the present work, an attempt was made to propose a new bronze considering the following information. The Cu-10.5%Al bronze is high tensile strength, but the material ductility is very low level, e.g., elongation to

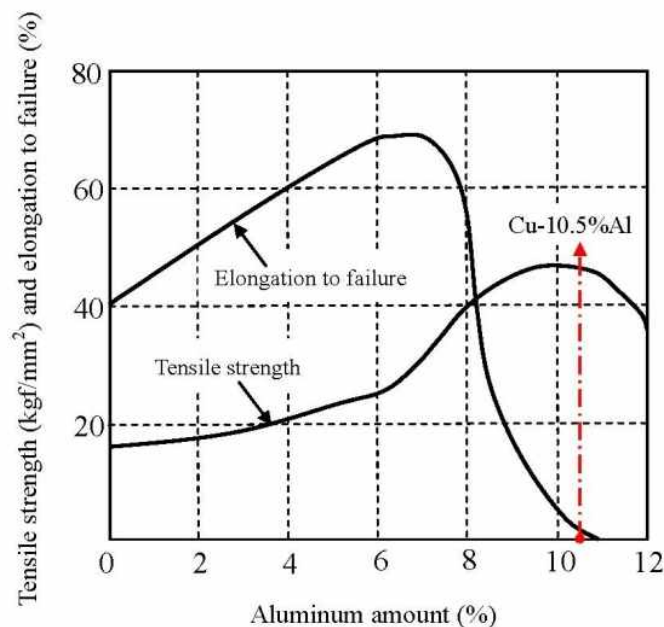


Fig. 1 Variation of tensile properties as a function of Al content in Cu

Table 1 Chemical composition of the CADZ, AIBC2 and HBsC3

	Al	Zn	Fe	Ni	Mn	Sn	Cn
CADZ	10.5		3.1	3.2	1.1	3.7	Bal.
AIBC ₂	9.3		3.8	2.0	0.8		Bal.
HBsC ₃	4.0	25.0	3.0		3.8		Bal.

failure is $\approx 0\%$, see Fig. 1. To obtain high material ductility, 3.7% Sn was added to Cu-10.5% Al. The related experimental data is shown in Ref. (Okayasu 2012). In addition, to obtain tiny microstructure, the proper amount of Fe and Ni (Fe/Ni = 0.89) was added, which makes tiny κ phase distributed in the matrix.

2. Experimental procedures

2.1 Material preparation

In the present work, a new bronze (CADZ) and two other commercial copper alloys, e.g., bronze (AIBC2) and brass (HBsC3), were used. The CADZ sample consists of Fe, Al, Sn and Ni, and is designed based on Cu-10.5%Al bronze with added several elements to make high mechanical properties as mentioned above (The Japan Society for Heat Treatment, The Japan Society for Heata Treatment, Zaima *et al.*, Engineering Technology and Basic Copper and Copper Alloy). Their chemical compositions are summarized in Table 1. Note that the new bronze (CADZ) was originally developed by the engineers in Dozen-Kogyo Co. Ltd (Y. Manabe), which called DZ400. All samples were produced by conventional gravity casting into a metal mold, where the melts in crucible were poured into the mold directly using a ladle. This casting process was carried out at room temperature. The shape of samples is a simple rectangular block for manufacture of ingot.

2.2 Microstructural observation

Microstructural characteristics of the three Cu alloys were investigated by an optical microscope, a energy dispersive X-ray spectroscopy (EDX) and electron backscatter diffraction (EBSD). The sample surfaces for all observation were polished to mirror flatness in a vibropolisher using colloidal silica for about 2 hrs. EDX analysis was carried out at an acceleration voltage of 15 kV using a scanning electron microscope (SEM, S-4300 Hitachi) and an energy dispersive X-ray spectrometer (EDX, EMAX-7000 Horiba). EBSD analysis was executed using a high resolution electron JSM-7000F microscope (JEOL Ltd.) with the following conditions: accelerating voltage 15 kV, beam current 5 nA and step size 1 μm . Based upon the analysis of the EBSD patterns, the crystal orientations of the samples were analyzed using HKL Channel 5 software.

2.3 Tensile and fatigue tests

Tensile and fatigue tests were carried out at room temperature using an electro-servo-hydraulic system with 50 kN capacity. Rectangular dumbbell shape specimens were employed with

dimensions $w = 3 \text{ mm} \times l = 20 \text{ mm} \times t = 2 \text{ mm}$, which introduced by electro-discharge machining (EDM). The specimen surfaces were ground with 800 emery paper to reduce stress concentration. The loading speed for the tensile test was 1 mm/min to failure. The tensile-tensile fatigue properties were examined using the relationship between the stress amplitude and the cycle number to failure, i.e. the S-N relationship. The cyclic loading was conducted using a sinusoidal waveform at a frequency of 30Hz and a load ratio (P_{\min}/P_{\max}) of $R = 0.1$ up to 10^7 cycles. The maximum applied stresses were determined based on the ultimate tensile strength of the sample, e.g., 20~80% of σ_{UTS} .

2.4 Hardness measurements

To examine the material hardness, two different measurements, including Rockwell hardness and Vickers hardness, were conducted. The reason for the two different ways is to examine the hardness in macro- and micro-area of the samples. The sample surface was polished to a mirror status before the measurement. The Rockwell hardness and Vickers hardness measurements were executed using an ARK-F1000 (Akashi Co. Ltd) and a dynamic ultra-micro-hardness tester (DUH-211 Shimadzu), respectively. The indentation load for the ultra-micro-hardness test was 10 mN. The Martens hardness (HM) was obtained for the samples, which is defined as the maximum applied load, P_{\max} , divided by the contact area A

$$HM = \frac{P_{\max}}{A(h)} \quad (1)$$

In this case, the contact area $A(h)$ can be taken as

$$A(h) = \frac{3\sqrt{3} \tan(a)}{\cos(a)} h^2 \quad (1a)$$

where h is the penetration depth of the indicator, and a refers to the face angle of the indenter (115°). Substituting Eq. (1a) into Eq. (1) leads to an expression for the Martens hardness as follows:

$$HM \approx \frac{P_{\max}}{26.37h^2} \quad (2)$$

2.5 Wear test

In this work, wear test was carried out by an originally designed wear system, where a round plate with dimension $\phi 200 \text{ mm} \times 5 \text{ mm}$ made of a hardened high carbon steel with HRC60 was employed to examine the wear resistance of the samples. The specimens were pressed on to the rotating steel plate at 25 N. The steel plate was rotated at a rotation speed of 0.8 m/s. The wear tests were conducted for a length of 3 km. The wear resistance was evaluated using the wear value obtained by the following equations.

$$V = \frac{W_{\text{before}} - W_{\text{after}}}{\rho \times 10^3} \quad (3)$$

$$\rho = \frac{W_{\text{air}}}{|W_{\text{water}}|} \times \rho_0 \quad (3a)$$

where W_{before} is the sample weight before the wear test, W_{after} is the sample weight after the wear test, ρ is the density of the sample, W_{air} is the sample weight in air, W_{water} is the sample weight in water and ρ_0 is density of water.

3. Results and discussion

3.1 Microstructural characteristics

Fig. 2 shows optical micrographs of (a) CADZ, (b) AIBC2 and (c) HBSC3. All the micrographs were obtained from the middle section of the sample. The microstructure consists of a Cu based matrix and several eutectic structures. From the EDX analysis, several different phases were detected in each sample, e.g., Cu-based and Fe-based phases. The CADZ sample consists of the Fe-Ni-Cu phase (Area I), Cu-Ni-Sn phase (Area II) and Cu-Al phase (Area III). Such a Fe-based structure might be related to the $(\text{Fe,Ni})_3\text{Cu}$ of the hardened intermediate compound (Adabavazeh *et al.* 2012). All phases disperse homogeneously in the CADZ matrix with a significant amount of discrete and spherical Fe-based phase (The Japan Society for Heata Treatment, Zaima *et al.*, Engineering Technology and Basic Copper and Copper Alloy). The overall microstructure in CADZ is smaller than that for the other samples. On the other hand, AIBC2 consists of the eutectic Fe (Area I), Cu-Al-Ni phase (Area II) and Cu-Al phase (Area III); and HBSC3 consists of the eutectic Fe (Area I), Cu-Zn-Al phase (Area II) and Cu-Zn phase (Area III). The grain size of Area III was measured, e.g., 3.30 μm (CADZ), 5.78 μm (AIBC2) and 4.73 μm (HBSC3). In this case, the grain size was determined by the mean value of more than 50 measurement data.

To understand the mechanical properties of the copper alloys, a Rockwell hardness was measured (Fig. 3). The Rockwell hardness obtained in the CADZ sample is HRB 90, which is greater than that in the AIBC2 (HRB 61) and HBSC3 (HRB 69) samples. To understand the details of the hardness properties, the hardness measurement was further executed in a tiny area using the dynamic ultra-micro-hardness tester. In this case, the hardness test was conducted in each phase (Areas I, II and III). Fig. 4 shows the results of the Martens hardness in each phase, shown in Fig. 2, and their indentation load-depth curves. Note, the hardness data is reflected by the profile of the load vs. depth relations (the maximum depth). In Area I, the hardness (about 3200 N/mm^2) in Fe base phase (CADZ) is almost same level compared to the Fe base structures in AIBC2 and HBSC3. In Area II, the hardness (2400 N/mm^2) in the Cu-Ni-Sn phase (CADZ) is more than 10% higher than that in the phases in other samples: Cu-Ni-Al phase (AIBC2) and Cu-Zn-Al phase (HBSC3). In Area III, the hardness of 1500 N/mm^2 in the Cu-Al phase (CADZ) is slightly higher than the related phase for AIBS2 and Cu-Zn phase for HBSC3. Such high hardness in the CADZ sample would be affected by tiny grains and the internal stress. The later one will be discussed in the later section of this paper. One of the authors has investigated the relationship between the grain size and the hardness although different alloys were used, where the lager the grain, the lower the hardness (Okayasu *et al.* 2012). Such a difference in the hardness properties could make different tensile strength and fatigue strength.

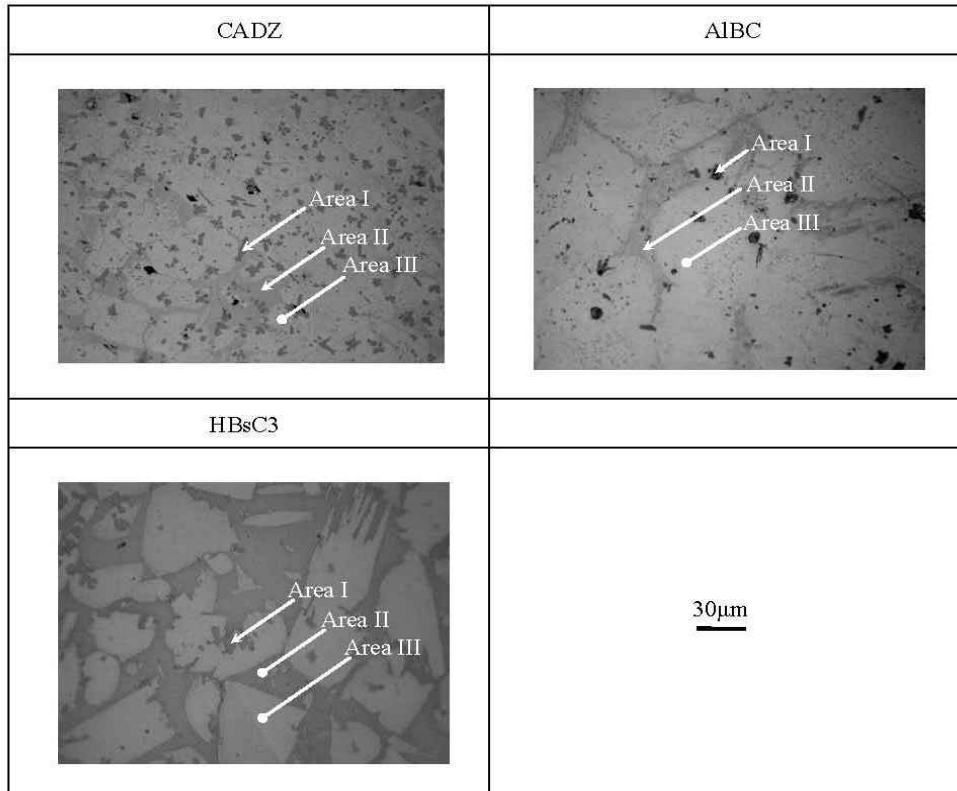


Fig. 2 Optical micrographs of the CADZ, AIBC2 and HBsC3 samples

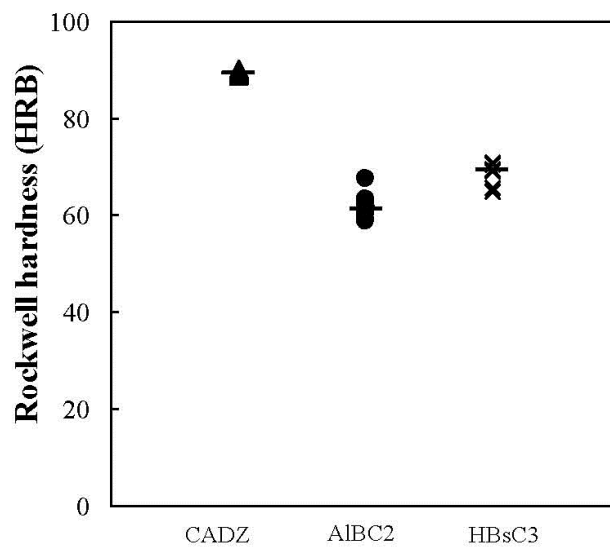


Fig. 3 Rockwell hardness of the CADZ, AIBC2 and HBsC3

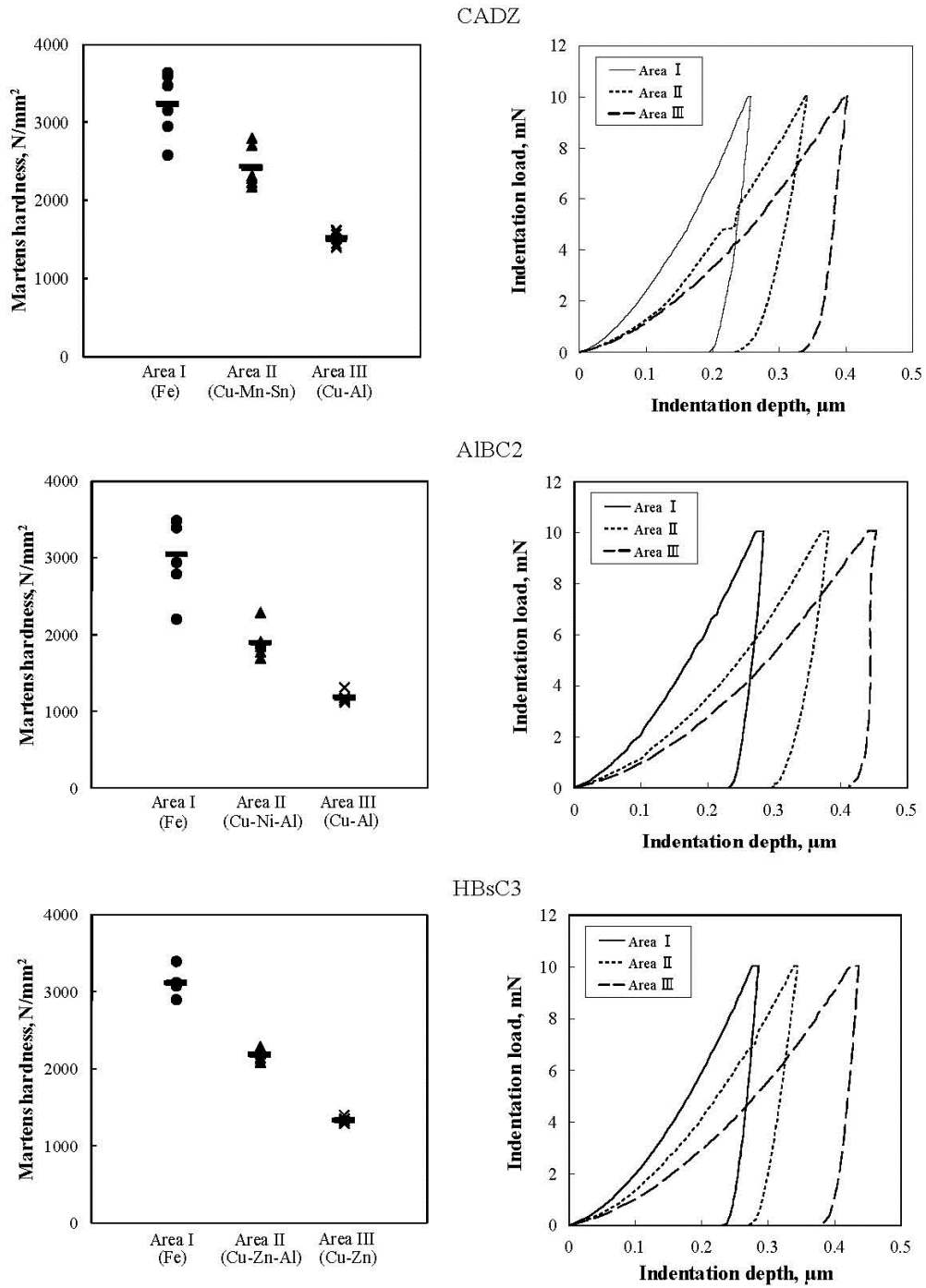


Fig. 4 Martens hardness in each microstructural phase (Area I, II and III) in the CADZ, AIBC2 and HBSc3 samples, and their indentation load-depth curves

3.2 Tensile and fatigue properties

The tensile and fatigue properties of all the samples were examined. Fig. 5 shows representative stress–strain curves. It can be seen that the tensile strength and strain to failure are clearly different depending on the sample: higher strength and lower ductility are obtained in the CADZ sample compared to the others. Based upon the stress-strain relations, the tensile strength (σ_{UTS}) and strain to failure (ε_f) are summarized in Fig. 6. As can be seen, the average tensile strength (σ_{UTS}) of the CADZ sample is about 700 MPa, which is more than 17% higher than the values for the AIBC2 and HBSc3 samples. Such difference in their UTS is similar trend to that for the hardness data as mentioned above. On the other hand, the strain to failure of CADZ is 0.02~0.05, which is lower than that for the others. Note, the material ductility of CADZ is slightly improved compared to Cu-10.5%Al alloy. This can be influenced by the proper amount of Sn added to the bronze .

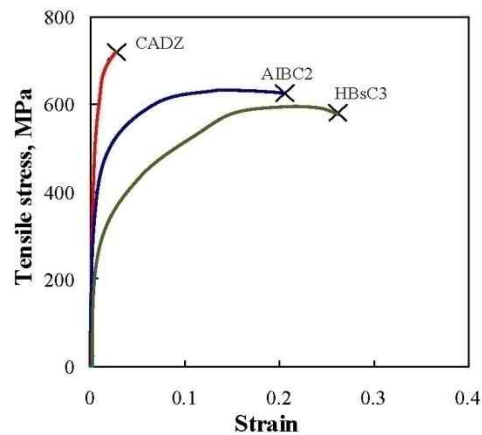


Fig. 5 Stress-strain curves for the CADZ, AIBC2 and HBSc3 samples

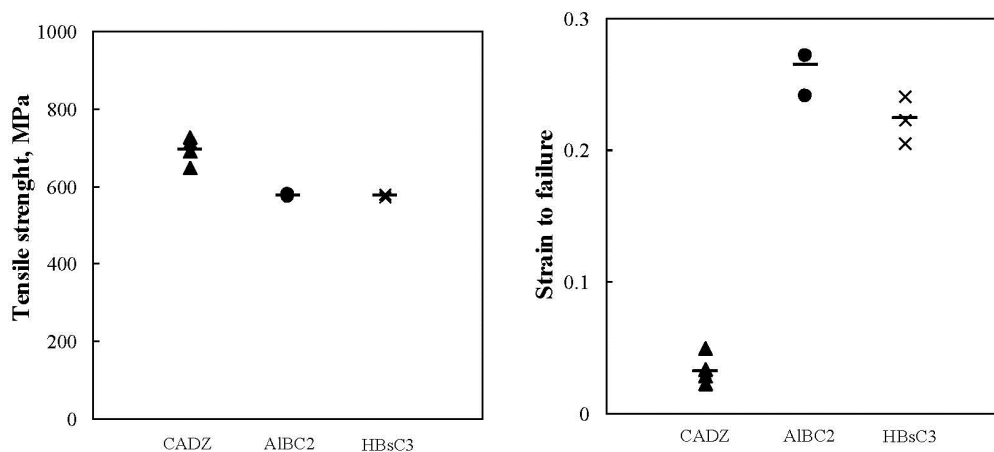


Fig. 6 Tensile properties of the CADZ, AIBC2 and HBSc3 samples

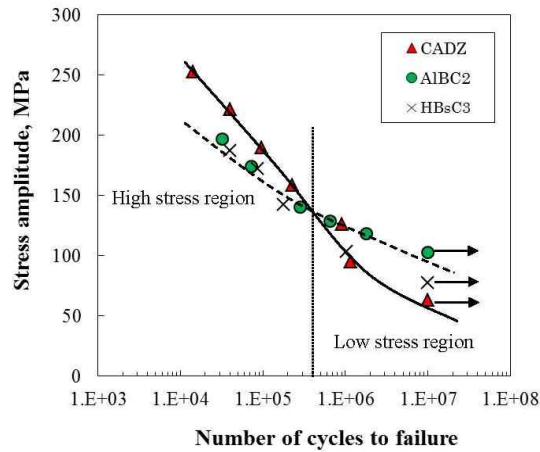


Fig. 7 Stress amplitude vs. cycles to failure for the CADZ, AIBC2 and HBSc3 samples

Fig. 7 shows the relationship between the stress amplitude and cyclic number to failure (S-N curve) for all samples. Note that the arrows in this figure indicate the specimens which did not fail within 10^7 cycles. The fatigue strength for the CADZ sample is slightly higher than that of AIBC2 and HBSc3 in the high stress region, while relatively lower fatigue strength at lower stresses, e.g., the endurance limit (σ_f) at 10^7 cycles for the CADZ sample is about 20% lower than the other samples. From the fatigue properties, the S-N relationship for CADZ crosses that for the other samples at around 5×10^5 cycles, as indicated by the hatching. Such S-N relationships might be attributed to different tensile properties, e.g., the high tensile strength and the low ductility for the CADZ sample, as shown in Fig. 6. In fact, it is possible that high ductile materials make long live under low stress condition, and high strength materials are advantageous at high stresses and long lives. Similar fatigue properties are also observed in the previous work (Ericsson and Sandström 2003) where the heat treated aluminum alloys were employed. Because of the heat treatment process conducted in Al alloys, their material should have high hardness, which could have similar properties in our CADZ sample.

The S-N relations can be summarized by a power law dependence of the applied stress amplitude (σ_a) and cycle number to failure (N_f): $\sigma_a = \sigma_f N_f^b$ (MPa), where σ_f is the fatigue strength coefficient and b is the fatigue exponent. The values of σ_f and b , obtained by least squares analysis, were (i) for the CADZ sample: $\sigma_f = 2183$ MPa and $b = -0.217$, (ii) for the AIBC2 sample: $\sigma_f = 985$ MPa and $b = -0.154$, and (iii) for the HBSc3 sample: $\sigma_f = 1075$ MPa and $b = -0.165$. In this case, high fatigue strength is expected for a high coefficient σ_f . The σ_f value for the CADZ sample was closed to that of the hardened SAE1045, i.e., $\sigma_f = 2725$ MPa (Hertzberg 1996).

3.3 Microstructural analysis

In order to interpret the effects of the microstructural characteristics on the mechanical properties, EBSD analysis was executed. Fig. 8 depicts the image quality map and the crystal orientation maps of the microstructure of the three samples. Different color in the crystal

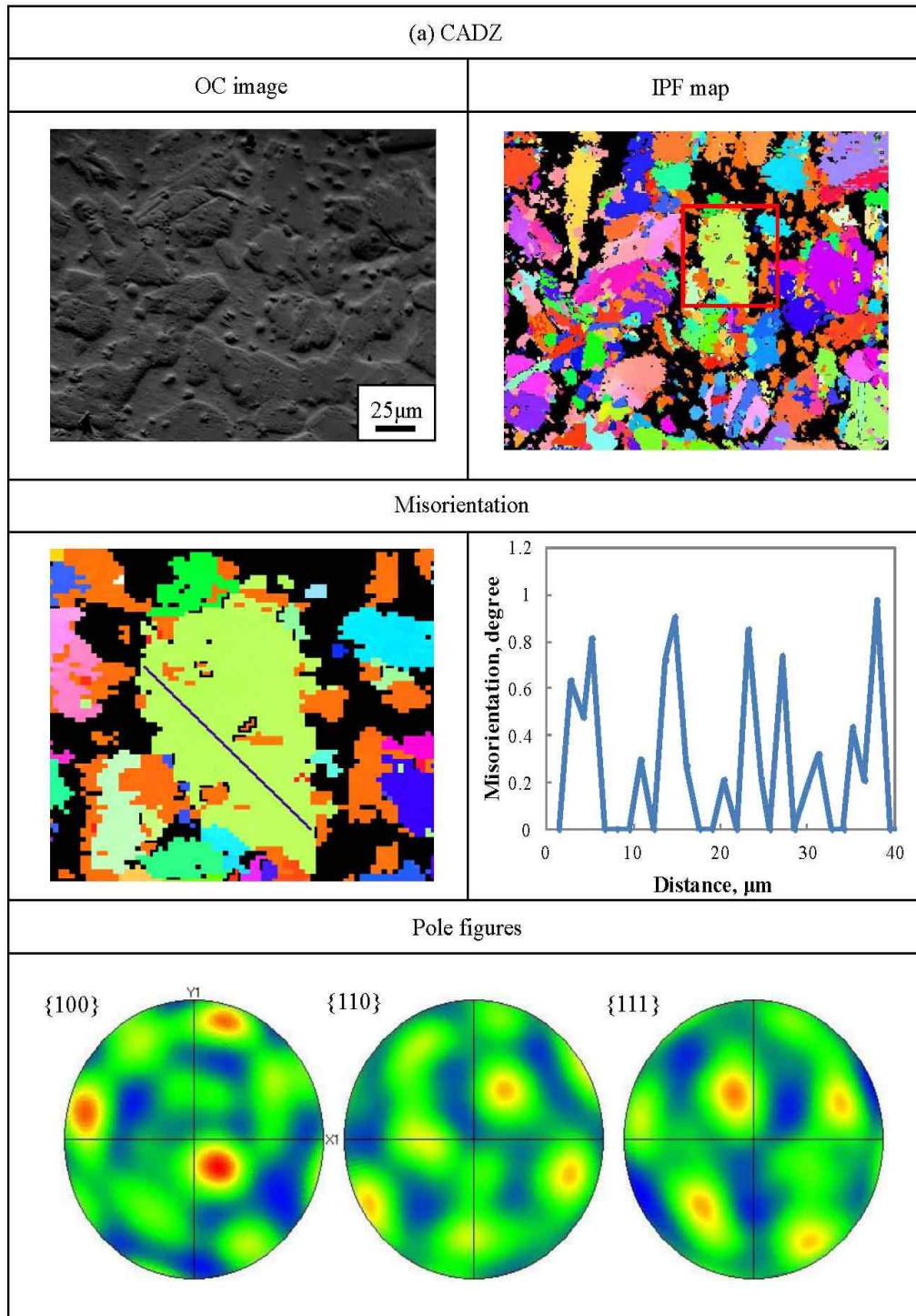


Fig. 8 Crystal orientation map with pole figures for $\langle 001 \rangle$, $\langle 100 \rangle$ and $\langle 110 \rangle$ poles and misorientation profile in a grain for the CADZ, AIBC2 and HBSc3 samples

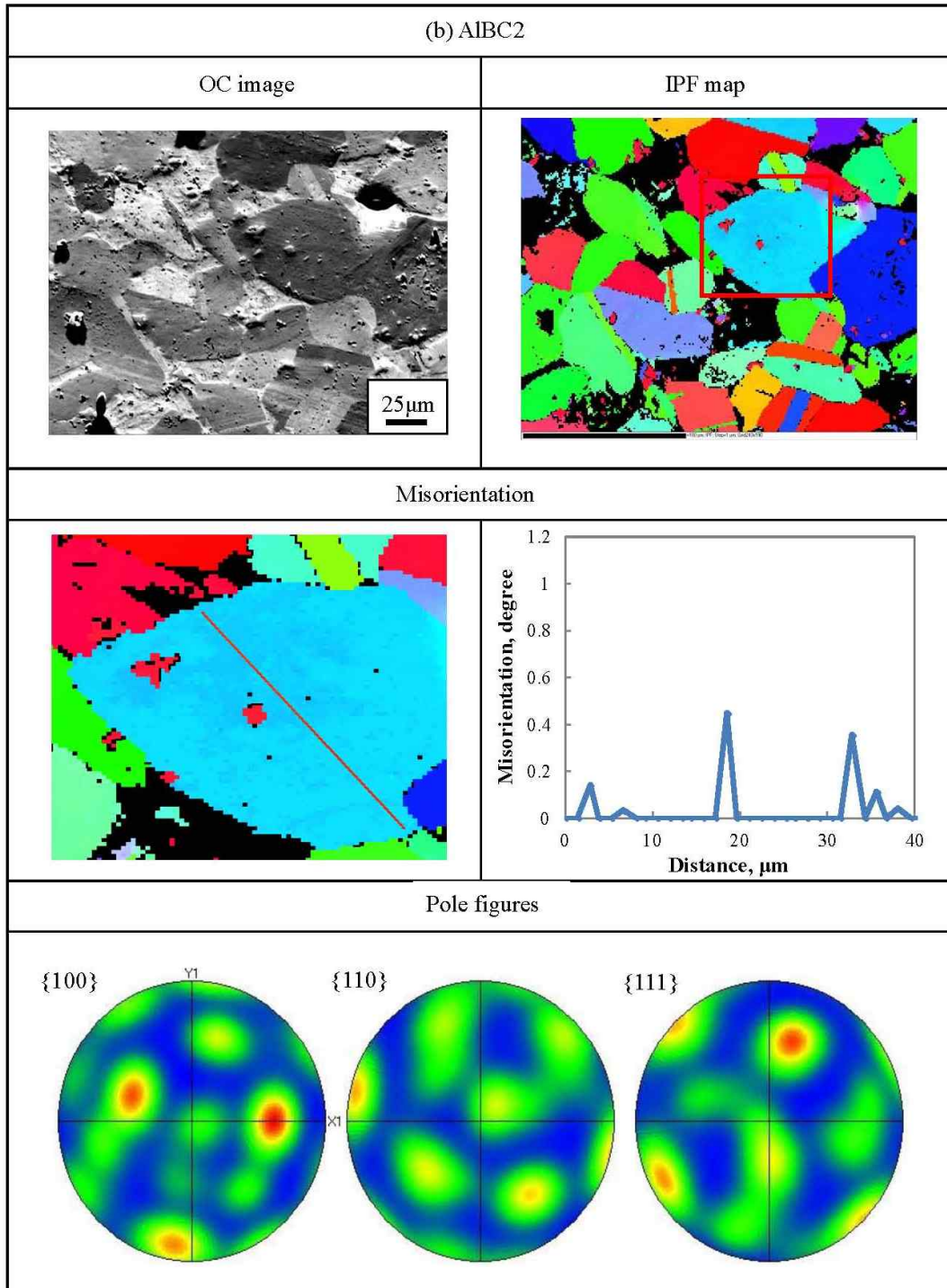


Fig. 8 Continued

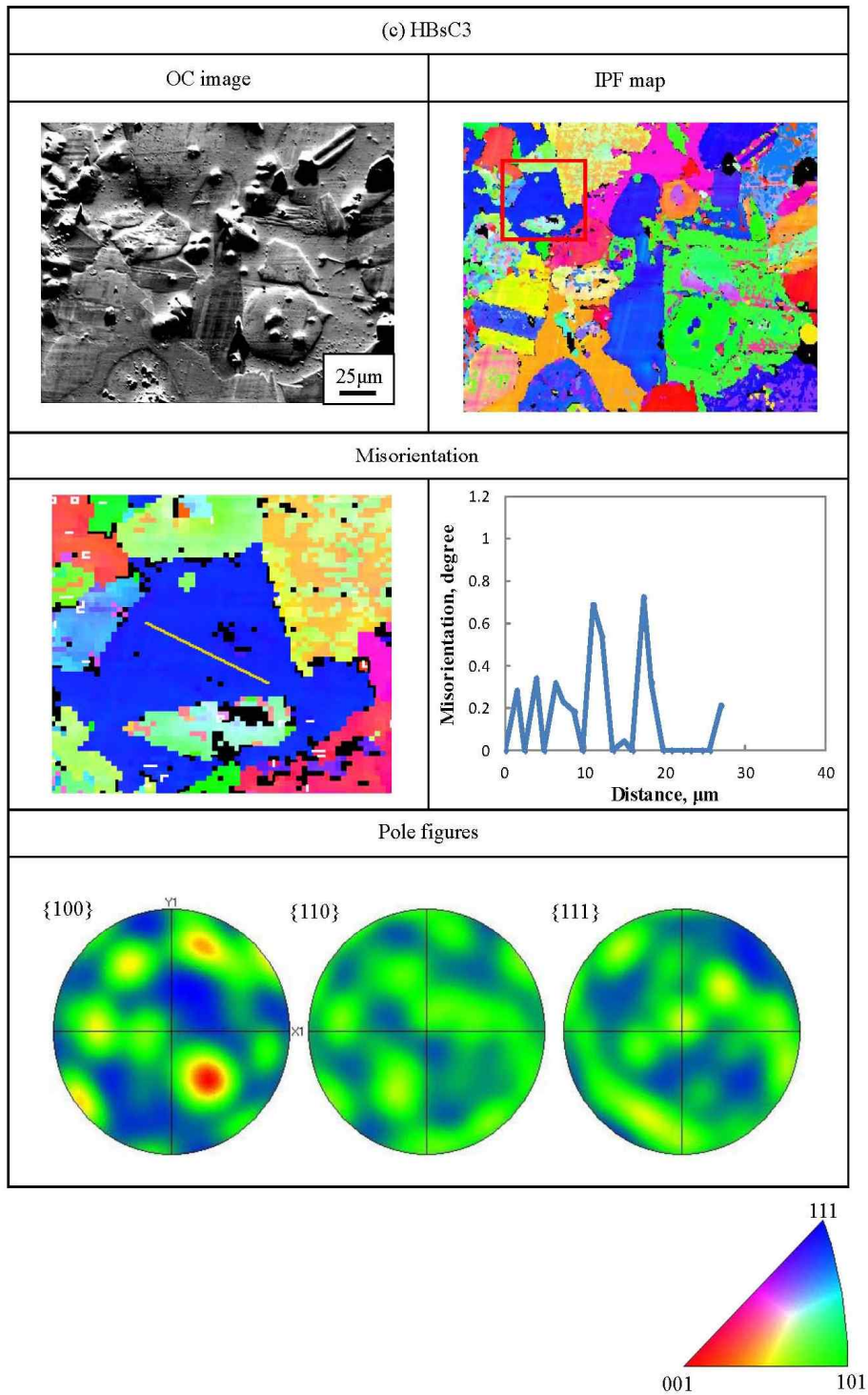


Fig. 8 Continued

orientation map is defined by the deviation of the measured orientation, as pointed in the stereographic projection. It is clear that crystal orientations in each grain are varied for all samples. It is also clarified that the misorientation angle patterns in grain are different. As in Fig. 8, low misorientation angle is detected in AIBC2 and HBsC3 although severer misorientation angle is obtained in the CADZ sample. Such high misorientation angle in CADZ may be created by complicated microstructure, which could produce high internal stress or high distortion energy (Littlewood *et al.*). Thus, the mechanical properties of the CADZ sample, e.g., the hardness and σ_{UTS} , are higher than the other ones.

3.4 Wear properties

The wear properties of all the cast copper alloys were investigated, and SEM image with EDX analysis is indicated in Fig. 9. It is seen that a wavy surface after the wear test can be seen in the SEM image. Interestingly, the relatively high dense of Fe element is detected on the wear surface as indicated by the dashed circle, which is affected by the hardened high carbon steel used for the wear test. Fig. 10 summarizes the amount of wear for all samples. It is interesting to note that the wear resistance varies depending on the sample. The mean wear value for CADZ is 0.034 mm^3 , which is more than 30% lower than that for the AIBC2 and HBsC3 samples. The reason for the improvement of wear resistance in CADZ can be caused by the high material hardness. In addition, the small Fe-based particle affects the high wear resistance, where a large number of Fe-based particles can make contact with the counterpart material. In this case, even though the total contact zone of Fe particles with the counterpart material is the similar level for all samples, irrespective of the size of the Fe particle, the small particles formed in CADZ contribute to increase the ultimate tensile strength, and consequently this alloy will show a decrease in specific wear (Hong and Suryanarayana 2005). From the above experimental results, the CADZ sample is capable of achieving the expected combination of mechanical strength and wear properties.

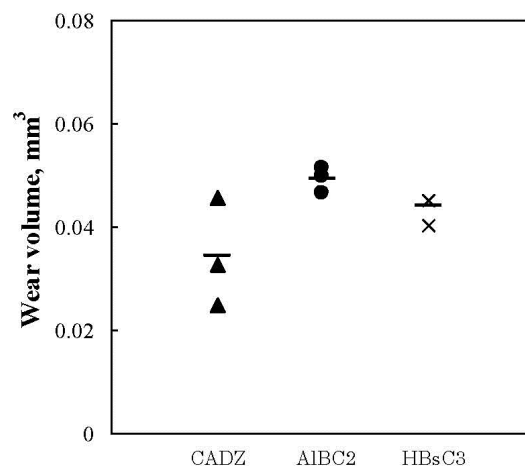


Fig. 9 EDX analysis for the CADZ sample around the wear surface taken by scanning for Cu and Fe

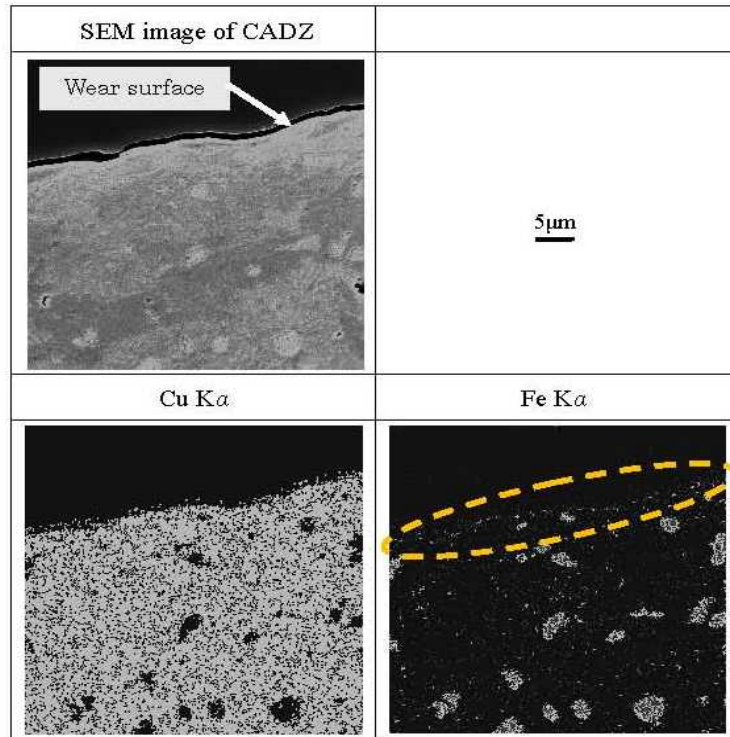


Fig. 10 Wear volumes for the CADZ, AlBC2 and HBsC3 samples

4. Conclusions

The mechanical and wear properties of the newly proposed bronze have been investigated experimentally. The results obtained can be summarized as follows:

1) The microstructure of the CADZ sample consists of Cu-Al-, Fe-Ni-Cu- and Cu-Ni-Sn-based phases. The material hardness of CADZ is much higher than that of the other copper alloys. Due to the high hardness of small Fe-based particles and other phase, excellent wear properties are obtained for the CADZ sample.

2) The material ductility of CADZ is lower than those for conventional bronzes. However, its ductility is slightly improved with addition of Sn element compare to Cu-10.5%Al alloy.

3) The fatigue strength for CADZ is higher than that for the other copper alloys in the high stress region, but there is a lower endurance limit due to the lower ductility for the CADZ sample.

Acknowledgements

The authors would like to express the appreciation to Dr. Noriko Muto at Akita Prefectural University and Mr. Kenya Matsumoto at Ehime University for their technical supports on the manuscript.

References

- Li, Y., Ngai, T.L. and Xia, X. (1996), "Mechanical, friction and wear behaviors of a novel high-strength wear-resisting aluminum bronze", *Wear*, **197**(1-2), 130-136.
- Waheed, A. and Ridley, N. (1994), "Microstructure and wear of some high-tensile brass", *J. Mater. Sci.*, **29**(6), 1692-1699.
- Li, W.S., Wang, Z.P., Lu, Y., Jin, Y.H., Yuan, L.H. and Wang, F. (2006), "Mechanical and tribological properties of a novel aluminum bronze material for drawing dies", *Wear*, **261**, 155-163.
- Kaplan, M. and Yildiz, A.K. (2003), "The effects of production methods on the microstructures and mechanical properties of an aluminum bronze", *Mater. Lett.*, **57**, 4402-4411.
- Adabavazeh, Z., Karimzadeh, F. and Enayati, M.H. (2012), "Synthesis and structural characterization of nanocrystalline (Ni,Fe)₃Al intermetallic compound prepared by mechanical alloying", *Adv. Powder Technol.*, **23**, 284-289.
- Turhan, H. (2005), "Adhesive wear resistance of Cu-Sn-Zn-Pb bronze with additions of Fe, Mn and P", *Mater. Lett.*, **59**, 1463-1469.
- The Japan Society for Heat Treatment, Nyuumon Kinzoku-Zairyo, Oga Shuppan. (in japanese)
- Zaima, S. Kinzoku-Zairyo, Asakura Shoten. (in japanese)
- Engineering technology and basic copper and copper alloy, Japan Copper and Brass Association. (in japanese)
- Okayasu M., Takasu S. and Mizuno M. (2012), "Relevance of instrumented nanoindentation for the assessment of the mechanical properties of eutectic crystals and α -Al grain in cast aluminum alloys", *J. Mater. Sci.*, **47**, 241-250.
- Ericsson, M. and Sandström, R. (2003), "Influence of welding speed on the fatigue friction stir welds and comparison with MIG and TIG", *Int. J. Fatigue*, **25**(12), 1379-1387.
- Hertzberg, R.W. (1996), *Deformation and fracture mechanics of engineering materials*, 4th Eds. John Wiley & Sons, Inc. New York.
- Littlewood, P.D., Britton, T.B. and Wilkinson, A.J. (2011) "Geometrically necessary dislocation density distributions in Ti-6Al-4V deformed in tension", *Acta Mater.*, **59**(16), 6489-6500.
- Hong, S.J. and Suryanarayana, C. (2005) "Mechanical properties and fracture behavior of an ultrafine-grained Al-20 wt pct Si alloy", *Metall. Mater. Trans. A*, **36A**, 715-723.